

## ARTICLE

# Translational Model-Informed Dose Selection for a Human Positron Emission Tomography Imaging Study of JNJ-54175446, a P2X7 Receptor Antagonist

Yan Xu<sup>1,\*</sup>, Xin Miao<sup>1</sup> , Paulien Ravenstijn<sup>2</sup>, Anja Hijzen<sup>3</sup>, Mark E. Schmidt<sup>3</sup>, Partha Nandy<sup>4</sup> and Honghui Zhou<sup>1</sup>

Positron emission tomography (PET) provides useful information in target engagement or receptor occupancy in the brain for central nervous system (CNS) drug development, however, dose selection for human PET studies is challenging and largely empirical. Here, we describe a translational pharmacokinetic/pharmacodynamic (PK/PD) modeling work to inform dose selection for a human PET study of JNJ-54175446, a CNS-penetrating P2X7 receptor antagonist. Models were developed using data on monkey brain occupancy and plasma drug exposures from a monkey PET study and early human clinical studies that provided data on drug exposures and human *ex vivo*-stimulated peripheral interleukin (IL)-1 $\beta$  release. The observed plasma PK of JNJ-54175446 in human was adequately described by a one-compartment model with parallel zero-order and first-order absorption and first-order elimination. An exposure-occupancy model was extrapolated from monkey to human assuming a similar unbound potency (all other model parameters remained unchanged). This model was then used to simulate human brain occupancy to guide human PET study dose selection, together with the human population PK model. The corroboration of model predicted occupancy by the observed occupancy data from the human PET study supports the use of a monkey as a predictive model for human PET target engagement. Potency estimate for brain occupancy was generally comparable to that for the suppression of the provoked peripheral IL-1 $\beta$  release *ex vivo*, indicating that blood IL-1 $\beta$  release may be used as a surrogate of central occupancy for JNJ-54175446. Translational PK/PD modeling approach could be used for selecting optimal doses for human PET and other clinical studies.

## Study Highlights

### WHAT IS THE CURRENT KNOWLEDGE ON THE TOPIC?

A human positron emission tomography (PET) study provides useful information for brain occupancy, however, its dose selection is challenging and largely empirical.

### WHAT QUESTION DID THIS STUDY ADDRESS?

Translational pharmacokinetic/pharmacodynamic modeling was conducted to guide dose selection for the human PET study of JNJ-54175446 (a P2X7 receptor antagonist) using data from early human clinical studies and a monkey PET study, including drug plasma exposure, human peripheral biomarker, and monkey brain occupancy.

### WHAT DOES THIS STUDY ADD TO OUR KNOWLEDGE?

The study demonstrated a successful model-informed dose selection for the human PET study.

Model-predicted P2X7 receptor occupancy in the human brain was overall consistent with what were observed clinically.

### HOW MIGHT THIS CHANGE CLINICAL PHARMACOLOGY OR TRANSLATIONAL SCIENCE?

Earlier introduction of PET study in monkey may provide valuable information in drug receptor binding in the brain and allow for quantitative model-informed dose selection for human PET studies and other clinical trials in neuroscience. Furthermore, this approach may reduce the number of subjects needed in clinical PET studies leading to shortened studies with reduced total cost.

JNJ-54175446 is an orally bioavailable, central nervous system (CNS)-penetrating, high affinity P2X7 receptor antagonist,<sup>1</sup> currently in development for the treatment of mood disorders. P2X7 receptor is an adenosine

triphosphate (ATP)-gated ion channel predominantly expressed on macrophages and monocytes in periphery, and microglia and astrocytes in the CNS.<sup>2,3</sup> In both the CNS and periphery, P2X7 receptor activation is associated with

Yan Xu, Xin Miao, and Paulien Ravenstijn contributed equally to this paper.

<sup>1</sup>Clinical Pharmacology and Pharmacometrics, Janssen Research & Development, LLC, Springhouse, Pennsylvania, USA; <sup>2</sup>Clinical Pharmacology and Pharmacometrics, Janssen Research & Development, LLC, Beerse, Belgium; <sup>3</sup>Neuroscience Experimental Medicine, Janssen Research & Development, LLC, Beerse, Belgium; <sup>4</sup>Clinical Pharmacology and Pharmacometrics, Janssen Research & Development, LLC, Titusville, New Jersey, USA. Correspondence: Yan Xu (yxu115@its.jnj.com)

Received: June 24, 2019; accepted: August 30, 2019. doi:10.1111/cts.12711

inflammasome activation leading to the production of the pro-inflammatory cytokines, such as interleukin (IL)-1 $\beta$ .<sup>4</sup> P2X7 receptor is hypothesized to be critical in mediating brain inflammation and CNS neuron-glia signaling leading to neurodegenerative and psychiatric diseases.<sup>5-7</sup>

JNJ-54175446 has been tested in single ascending dose (SAD; NCT02475148)<sup>8</sup> and multiple ascending dose (MAD; NCT02515955) studies in healthy subjects and is well-tolerated up to 600 mg single dose and 450 mg once daily following oral administration. The median time to achieve maximal concentration ( $T_{max}$ ) ranged from 2–4 hours under fasted conditions, and the elimination half-life was ~ 35 hours. JNJ-54175446 demonstrated nonlinear pharmacokinetics (PKs) with less than dose proportional increase in exposure over the dose range tested. Food effect was shown with higher exposure under fed compared with fasted condition. Passive CNS penetration was confirmed as drug concentrations in cerebrospinal fluid corresponded well to the free drug concentrations in plasma.<sup>8</sup>

The development of drugs for CNS diseases is often impaired by the lack of appropriate animal model and quantifiable markers of drug effect that are relevant to the human condition. The pharmacodynamic (PD) effect of JNJ-54175446 has been evaluated in healthy subjects by assessing IL-1 $\beta$  release following *ex vivo* stimulation of human blood with lipopolysaccharide (LPS) and 3'-O-(4-benzoylbenzoyl)-ATP (BzATP). Results indicated an approximately full and continuous antagonism of IL-1 $\beta$  stimulation at doses  $\geq$  50 mg/day. To confirm target engagement and define the exposure-receptor occupancy (RO) relationship in the brain, a positron emission tomography (PET) study (NCT03088644)<sup>9</sup> was planned for JNJ-54175446 with [<sup>18</sup>F]-JNJ-64413739, a P2X7 receptor-specific PET tracer. A measure of target engagement can be obtained by assessing the extent of competitive binding, or occupancy, by the drug.<sup>10</sup> However, it is challenging to predict

brain exposure and occupancy for human PET studies. The radiation burden associated with PET scans and complexity of radiolabeling of tracers developed for research use limit the number of scans that can be conducted, driving a need to optimize dose selection.<sup>11</sup>

Here, we describe translational PK/PD modeling work to inform dose selection for the human PET study of JNJ-54175446 by leveraging existing monkey and human data. Specifically, a stepwise modeling and simulation approach was used (Figure 1), including human population PK/PD (step 1), monkey exposure-brain P2X7 RO analysis and extrapolation to human (step 2), simulation of human brain RO with integrated human population PK and occupancy model derived from the monkey PET, and further model validation using clinical observations when available (step 3).

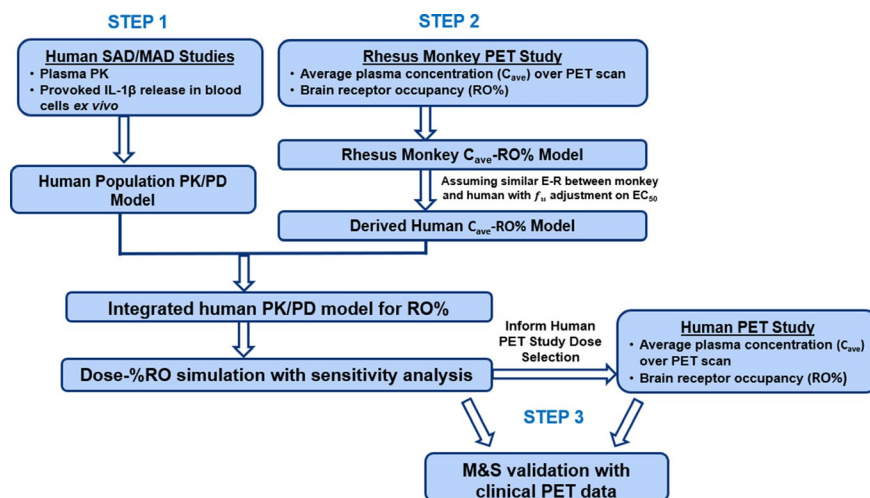
## METHODS

### Human study design and sample collection

The study designs for the SAD (NCT02475148)<sup>8</sup> and MAD (NCT02515955) studies and the [<sup>18</sup>F]-JNJ-64413739 PET study (NCT03088644)<sup>9</sup> have been described elsewhere and briefly summarized below and in Table S1. Protocols were approved by the investigational review board or ethics committee and all subjects provided written informed consent.

All doses of JNJ-54175446 in SAD and MAD studies were administered orally as a liquid formulation in healthy subjects, including single 0.5–300 mg doses under fasted conditions, single 50–600 mg doses with high-fat meals, and 50–450 mg once daily for 10 days with standard meals. For human population PK/PD analysis, data included blood samples for PK and *ex vivo* IL-1 $\beta$  release from SAD/MAD studies, as shown in Table S1.

The human PET study was an open-label study to measure the changes of [<sup>18</sup>F]-JNJ-64413739 (PET tracer) kinetics



**Figure 1** Translational pharmacokinetic/pharmacodynamic (PK/PD) modeling work flow. *STEP 1*: Human population PK/PD model was developed with data from two phase I studies (single ascending dose (SAD) and multiple ascending dose (MAD)). *STEP 2*: Monkey exposure-brain receptor occupancy model was developed with data from a monkey PET study using average concentration during positron emission tomography (PET) scan as the exposure metric. The model was translated to human assuming a similar unbound potency. *Step 3*: Simulation of human brain occupancy was conducted using integrated human population PK model and the occupancy model derived from the monkey PET. The results were further validated using clinical observations when available.  $C_{ave}$ , average concentration during PET scan; M&S, modeling and simulation; RO, receptor occupancy.

in the brain at approximately  $T_{\max}$  (4–6 hours) following single oral doses of JNJ-54175446 (5–300 mg with standard meals) and to assess the exposure/receptor interaction of JNJ-54175446. Eight healthy men underwent a baseline PET scan, and two postdose scans (separated at least 1 week apart; **Table S1**). Data collected for the human exposure-occupancy modeling analysis included blood samples for PK (~ 4, 4.75, and 6 hours postdose, corresponding to immediately before tracer injection, midway through, and immediately upon completion of the scan, respectively) and RO data from the [ $^{18}\text{F}$ ]-JNJ-64413739 PET images.<sup>9</sup>

### Monkey PET study design and sample collection

The monkey PET study was performed at Molecular NeuroImaging (New Haven, CT) using protocols approved by the Institutional Animal Care and Use Committee.<sup>12</sup> One male (12.1 kg; received 3 single JNJ-54175446 doses) and one female (8.7 kg; received 2 single JNJ-54175446 doses) rhesus macaques (*Macaca mulatta*) received baseline, vehicle, or blockade scans prior to which JNJ-54175446 was administered intravenously (doses: 0.1, 0.4, 2.5, and 5.3 mg/kg), starting 10 minutes before [ $^{18}\text{F}$ ]-JNJ-64413739 injection. All experiments were performed on different days, spaced at least 2 weeks apart. Data collected for the monkey exposure-occupancy modeling analysis included blood samples for PK (~ 10 minutes, 70 minutes and 130 minutes postdose, corresponding to immediately before tracer injection, midway during, and immediately upon completion of the scan, respectively) and RO data obtained from PET images.

### Bioanalytical methods

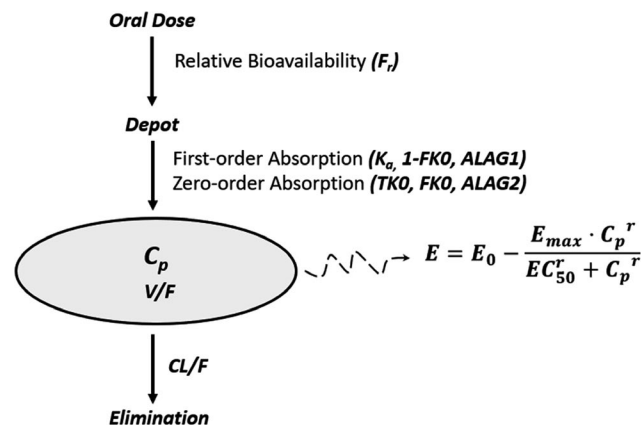
Plasma JNJ-54175446 concentrations were quantified using liquid chromatographic-mass spectrometry/mass spectrometry.<sup>8</sup> For SAD/MAD and PET studies, the lowest quantifiable concentration was 0.500 ng/mL and 2.50 ng/mL, respectively.

The analysis of IL-1 $\beta$  release from *ex vivo* LPS-primed BzATP stimulated peripheral blood cells has been described elsewhere.<sup>8</sup> Because IL-1 $\beta$  release measurement is based on two tubes (IL-1 $\beta$  level in the tube that contained only LPS subtracted from the IL-1 $\beta$  level in the tube that contained both LPS and BzATP), the value may be less than zero due to assay variability.

### Human population PK/PD model development

The human population PK/PD analysis utilized a pooled data set from SAD/MAD studies.

**Population pharmacokinetic model.** The base model was selected following comparisons of several structural models including one-compartment and two-compartment disposition with linear elimination and various absorption models, including zero-order and first-order absorption (with and without a lag time), and a combination of these features. Parallel zero-order and first-order input (**Figure 2**), depicting the absorption as a two-part process in which a fraction of the drug is absorbed (FK0) during a period of TK0 with a zero-order absorption and the remaining fraction of absorbable drug (1-FK0) is absorbed with a first-order absorption rate constant ( $K_a$ ), was found to best describe the



**Figure 2** Schematic representation of human final population pharmacokinetic/pharmacodynamic (PK/PD) model. The PK model developed is a one-compartment model with parallel zero-order and first-order absorption (with lag time) and first-order elimination. The PD model is a sigmoidal maximal drug effect achievable ( $E_{\max}$ ) direct-effect model linking drug plasma concentration to the inhibition of provoked IL-1 $\beta$  release in blood cells *ex vivo*. ALAG1, lag time for the first-order absorption; ALAG2, lag time for the zero-order absorption;  $C_p$ , plasma concentration; CL/F, apparent oral clearance;  $E_0$ , baseline IL-1 $\beta$  release;  $EC_{50}^r$ , concentration inducing 50% maximal drug effect;  $F_r$ , relative bioavailability when compared with the 150 mg dose under fasted condition; FK0, fraction of the dose absorbed by the zero-order process;  $\gamma$ , sigmoidal factor;  $K_a$ , first-order absorption rate constant, TK0, duration of input by the zero-order absorption process; V/F, apparent volume of distribution.

oral absorption characteristics of JNJ-54175446 (**Table S2**). The interindividual variability (IIV) of the PK parameters was described using a log-normal random effect model. The residual model explored included additive, proportional, and combined additive plus proportional error models.

To describe the dose-dependent nonlinearity and food effect on PK, an empirical parameter of relative bioavailability ( $F_r$ ) was introduced and the covariate effects of dose and food were tested for significance on  $F_r$  as follows:

$$F_r = F_r \cdot \exp\left(-\beta \times \left(\frac{\text{DOSE}}{150}\right)\right) \cdot E_{\text{FOOD}} \cdot \text{FOOD} \quad (1)$$

where  $F_r$  represents the relative bioavailability when compared with the 150 mg fasted dose ( $F_r = 1$  at 150 mg fasted dose), DOSE is the dose level in mg,  $\beta$  is the rate constant describing the dose effect on  $F_r$ , FOOD = 0/1/2 is the indicator for fasted/high-fat/standard meal conditions, and  $E_{\text{FOOD}}$  represents the food effect on  $F_r$ . As intravenous data were not available for JNJ-54175446, the absolute bioavailability could not be estimated.

Other covariates were evaluated on apparent clearance (CL/F), including body weight, age, and sex. Effect of body weight was also evaluated on apparent volume of distribution (V/F). Covariate selection was determined by the likelihood ratio test at the 5% significance level as well as clinical experience and overall model fits.

**Population PD model for *ex vivo*-stimulated IL-1 $\beta$  release inhibition.** Individual Empirical Bayesian parameter estimates based on the population PK model were used

in a sequential modeling approach<sup>13</sup> for modeling of IL-1 $\beta$  release inhibition. As *ex vivo*-stimulated IL-1 $\beta$  release is P2X7 receptor-dependent, a direct response sigmoidal maximal drug inhibition effect ( $E_{\max}$ ) model was used to link model-predicted drug concentration and IL-1 $\beta$  release as follows:

$$E = E_0 - \frac{E_{\max} \cdot C_p^\gamma}{EC_{50,IL1\beta}^\gamma + C_p^\gamma} \quad (2)$$

where  $C_p$  is concentration,  $E_0$  is baseline IL-1 $\beta$  release,  $E_{\max}$  is maximal drug inhibition effect,  $EC_{50,IL1\beta}$  is the concentration inducing 50% maximal drug inhibition, and  $\gamma$  is the sigmoidal factor ( $\gamma = 1$  for simple  $E_{\max}$  model).

IIV was assumed to be log-normally distributed for  $E_{\max}$  and  $EC_{50,IL1\beta}$ , and normally distributed for  $E_0$ . The residual model tested was an additive error model.

**Model evaluation.** Model selection was determined by graphical assessment, statistical significance, and model stability based on model convergence and condition number. The performance of the final model was further evaluated using visual predictive check ( $n = 1,000$  replicates).

#### Monkey exposure-brain occupancy model development and translation to human

Based on graphical exploration, relationship between average JNJ-54175446 plasma concentration over PET scan and brain occupancy was modeled as:

$$E = \frac{E_{\max} \cdot C_{\text{ave}}^\gamma}{EC_{50,RO}^\gamma + C_{\text{ave}}^\gamma} \quad (3)$$

where  $C_{\text{ave}}$  is the average concentration over PET scan,  $E_{\max}$  is the maximal drug effect achievable,  $EC_{50,RO}$  is the concentration inducing 50% maximal occupancy, and  $\gamma$  is the sigmoidal factor.

This exposure-occupancy model in monkey was then translated to human assuming a similar unbound  $EC_{50,RO}$  (all other model parameters remained unchanged) as shown below:

$$EC_{50,RO, \text{human}} = EC_{50,RO, \text{monkey}} \cdot \frac{f_{u, \text{monkey}}}{f_{u, \text{human}}} \quad (4)$$

where  $EC_{50,RO, \text{human}}$  and  $EC_{50,RO, \text{monkey}}$  are  $EC_{50,RO}$  in human and monkey, respectively,  $f_{u, \text{human}}$  and  $f_{u, \text{monkey}}$  are fractions unbound in human (11.2%) and monkey (17.0%), respectively. Such translation is considered reasonable, given the overall similar intrinsic *in vitro* potencies across species for JNJ-54175446.<sup>1</sup>

#### Model-based simulation to inform human PET study dose selection

The extrapolated human exposure-occupancy model together with the final population PK model was used to simulate P2X7 RO in human brain at 4–6 hours (approximate  $T_{\max}$ ) following single JNJ-54175446 doses of 5–600 mg. Sensitivity analyses were performed with a few tentative human  $EC_{50,RO}$  values (0.2-fold to 5-fold of derived human  $EC_{50,RO}$  using Eq. 4) to evaluate the impact on dose decision.

#### Translational model prediction vs. human PET study observations

Based on the translational model-informed dose selection, doses for the human PET study were selected. Observations from human PET studies were then compared with the model predictions. Using the same modeling approach described in Eq. 3, a human exposure-occupancy model was also developed, and the results were compared with those developed in monkey PET.

#### Software

Nonlinear mixed-effects modeling were conducted using NONMEM (version 7.4, ICON). The first-order conditional estimation with interaction was used for all model runs. Diagnostic graphics and postprocessing of the modeling outputs were performed using R software (version 3.4.1).

#### RESULTS

##### Human population PK/PD model analysis results

The population PK analysis included 2,560 plasma JNJ-54175446 concentrations from 107 healthy subjects who received at least 1 dose of JNJ-54175446 and had at least 1 postdose concentration measurement. The median age of subjects was 31 years (range 18–69 years) and the median body weight was 77.3 kg (range 46.5–113.4 kg). The majority of subjects was white (87%; 93 of 107) and men (97%; 104 of 107). All doses were administered orally as a liquid formulation, with 39% of subjects (42 of 107) under fasted condition, 16% of subjects (17 of 107) with a high-fat meal, and 45% of subjects (48 of 107) with a standard meal.

**Figure 2** provides the schematic of final population PK/PD model (see **File S1** for example model code). The PK model developed was a one-compartment model with parallel zero-order and first-order absorptions (with lag time) and first-order elimination. Compared with the separate zero-order or first-order input, the combined absorption model provided better model fits (objective function value drops of 44 to over 1,000; see **Table S2** for key model comparison). The final PK model had IIV for  $K_a$ , CL/F, V/F, and proportional residual error. Dose-dependent nonlinearity and food effect on PK were incorporated to the relative bioavailability  $F_r$ . In addition, body weight was identified as a covariate for CL/F and V/F.

**Table 1** lists the final PK model parameter estimates. All parameters were estimated reasonably well with relative standard errors < 30% for most parameters. The typical CL/F and V/F in healthy subjects weighing 70 kg following 150 mg oral dose under fasted condition were 5.10 L/hour and 272 L, respectively. The majority of the oral dose (92.4%) was absorbed via the first-order absorption route and only a small fraction (7.6%) via the zero-order absorption route. The first-order absorption rate constant ( $K_a$ ) was 0.428 hour<sup>-1</sup> and the duration of the zero-order process (TK0) was 1.05 hour. CL/F and V/F increased nonlinearly with body weight. Subjects who received higher dose tended to have a lower relative bioavailability and, thus, lower exposure when normalized by dose. Compared with subjects who received JNJ-54175446 under fasted conditions, subjects with high-fat and standard meals had a higher bioavailability (76% and 63% higher, respectively).

**Figure 3** shows the visual predictive check results of the final population PK model. The model described the data

**Table 1** Parameter estimates in the final population PK and PD model in human

Parameters <sup>a</sup>	Description	Estimate <sup>b</sup>
PK parameters		
CL/F (L/hour) <sup>c,d</sup>	Apparent clearance	5.10 (4.77)
BWT on CL/F	Body weight effect on apparent clearance	0.426 (47.6)
V/F (L) <sup>d,e</sup>	Apparent volume of distribution	272 (3.56)
BWT on V/F	Body weight effect on apparent volume of distribution	1.14 (12.5)
TK0 (hour)	Duration of input by the zero-order process	1.05 (29.6)
FK0	Fraction of the dose absorbed by the zero-order process	0.0760 (35.7)
K <sub>a</sub> (1/hour)	First-order absorption rate constant	0.428 (10.8)
ALAG1 (hour)	Lag time for first order process	0.287 (8.58)
ALAG2 (hour)	Lag time for zero order process	2.03 (0.0343)
F <sub>r</sub> <sup>f</sup>	Relative bioavailability (150 mg, fasted)	1 (fixed)
β (1/hour)	Rate by which F <sub>r</sub> changes with dose	0.178 (11.2)
E <sub>FOOD</sub> (FOOD = 2)	Effect of high-fat food on F <sub>r</sub>	1.76 (6.10)
E <sub>FOOD</sub> (FOOD = 1)	Effect of regular food F <sub>r</sub>	1.63 (4.70)
IIV of V/F (CV%)	IIV of apparent volume of distribution	19.8% (16.2) [5.54] <sup>b</sup>
IIV of CL/F (CV%)	IIV of apparent clearance	30.0% (15.0) [1.61] <sup>b</sup>
IIV of K <sub>a</sub> (CV%)	IIV of first-order absorption rate constant	104% (13.8) [2.11] <sup>b</sup>
Proportional residual error (CV%)	—	17.5% (3.92)
PD parameters		
E <sub>0</sub> (pg/mL)	Baseline ex vivo stimulated IL-1β release	798 (2.50)
E <sub>max</sub> (pg/mL)	Maximal effect of inhibition	747 (1.76)
EC <sub>50,IL1β</sub> (μg/mL)	Concentration inducing 50% of maximal inhibition in IL-1β release	0.0670 (12.5)
IIV of E <sub>0</sub>	IIV of baseline ex vivo IL-1β release	206 (8.36) [5.62] <sup>b</sup>
IIV of EC <sub>50,IL1β</sub> (CV%)	IIV of concentration inducing 50% of maximal inhibition in IL-1β release	44.9% (55.1) [66.4] <sup>b</sup>
Additive residual error (pg/mL)	—	199 (0.966)

CV%, percentage of coefficient of variation; IIV, interindividual variability; PD, pharmacodynamic; PK, pharmacokinetic.

<sup>a</sup>IIV = interindividual variability calculated as (variance)<sup>1/2</sup> × 100%. <sup>b</sup>Mean (% relative standard error) [shrinkage %] estimates. <sup>c</sup>CL/F ( $\frac{L}{h}$ ) = 5.10 × ( $\frac{BWT}{70}$ )<sup>0.426</sup>. <sup>d</sup>Typical CL/F and V/F estimates in typical healthy subjects with body weight of 70 kg following 150 mg oral dose under fasted condition. <sup>e</sup>V/F (L) = 272 × ( $\frac{BWT}{70}$ )<sup>1.14</sup>. <sup>f</sup>F<sub>r</sub> = F<sub>r</sub> × exp(-β × ( $\frac{Dose}{150}$ )) × E<sub>FOOD</sub> × FOOD.

reasonably, although less optimal for low doses at the absorption phase. At 0.5 and 2.5 mg, the model predicted maximal concentration (C<sub>max</sub>) tended to be lower than observed. Nevertheless, model fits seemed to be adequate at doses ≥ 50 mg where apparent PD effects were observed. Additional diagnostic plots were assessed, and no appreciable bias was identified (**Figure S1**).

The JNJ-54175447 plasma concentration-related reduction in provoked IL-1β release in blood cells ex vivo was described with an E<sub>max</sub> model (parameter estimates in **Table 1**). The concentration inducing EC<sub>50,IL1β</sub> release was 67 ng/mL with relative standard error of 12.5%, indicating robust potency estimation. The performance of the final PD model was assessed through the superposition of the observed IL-1β and the simulated median trend. It suggests that the model reasonably described the observed IL-1β release inhibition.

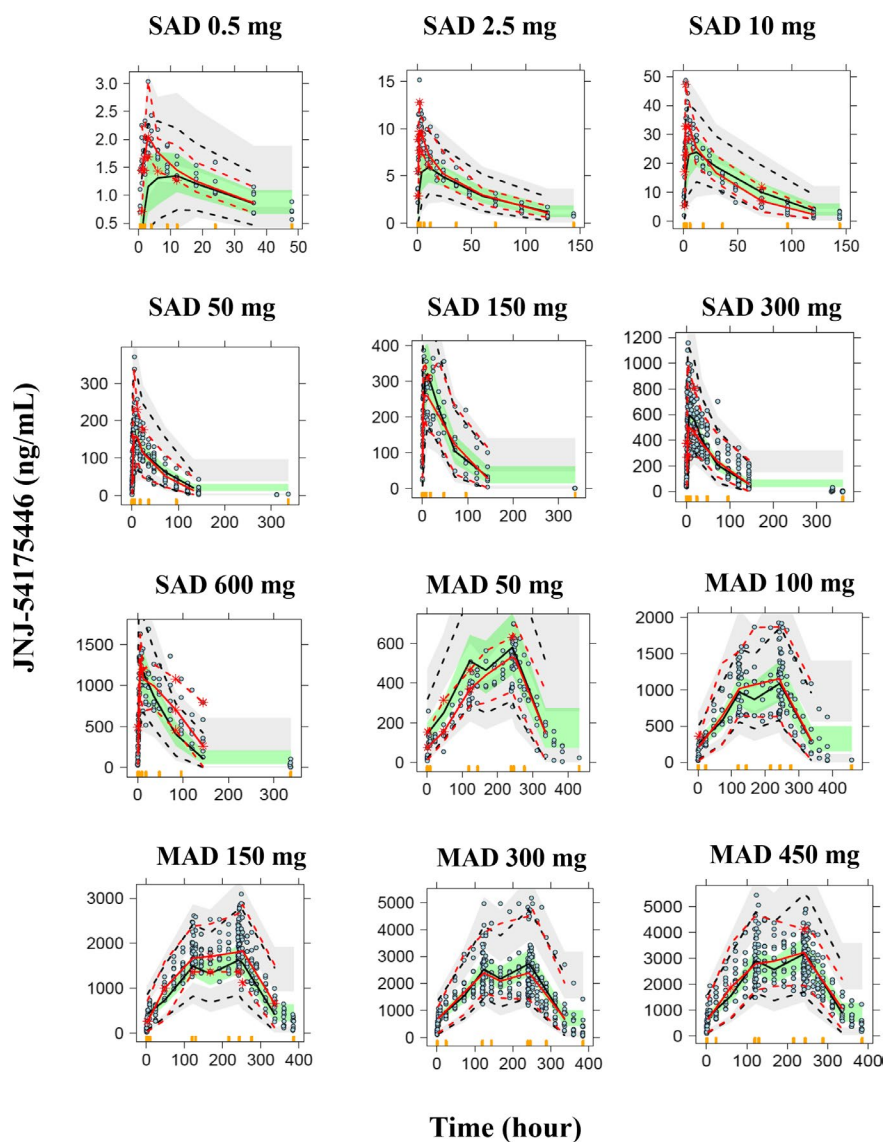
### Monkey exposure-brain occupancy modeling analysis results and translation to human

A total of five occupancy measures from two rhesus monkeys (single intravenous JNJ-54175446 doses from 0.1 to 5.3 mg/kg) were collected to assess the monkey exposure-brain occupancy relationship using average plasma concentration over PET scan. A sigmoidal E<sub>max</sub> model was

developed and the results are shown in **Table 2** (parameter estimates) and **Figure 4a** (overlay of observed vs. simulated). The estimated maximal brain occupancy (E<sub>max</sub>) was 56.0% and the potency (EC<sub>50,RO</sub>) was 43.2 ng/mL. Assuming a similar unbound EC<sub>50,RO</sub> between human and monkey, the derived EC<sub>50,RO</sub> in human was 65.6 ng/mL, after taking into account differences in fraction unbound between human and monkey (Eq. 4).

### Model-based simulation and human PET study dose selection

The final human population PK model integrated with the extrapolated human exposure-occupancy model from a monkey PET was used to simulate brain occupancy in human at 4–6 hours postdose following single JNJ-54175446 doses of 5–600 mg, including a sensitivity analysis on the derived human EC<sub>50,RO</sub>. At all simulated potency values (i.e., 0.2-fold to 5-fold of derived EC<sub>50,RO</sub>, or 13–325 μg/mL), the maximal RO would be reached at a dose of 150 mg (**Figure 4b** and **Table S3**). Hence, 150 mg was selected as a first dose to be tested in the human PET study. A 2-fold higher dose than 150 mg (i.e., 300 mg) was selected as a second dose to confirm whether maximal RO in human had been reached with 150 mg. In human, single doses up to 600 mg have been



**Figure 3** Observed vs. predicted for final population pharmacokinetic model stratified by study and treatment group. Blue points are the observed individual data. Red solid and dashed lines are the 50th and 5th/95th percentile of the observations. Black solid and dashed lines are the 50th and 5th/95th percentile of the model predictions. Green areas are the 90% confidence interval (CI) of the simulated median trend. Gray areas are the 90% CI of the simulated trends at 5th and 95th percentiles. MAD, multiple ascending dose study; SAD, single ascending dose study.

tested and found to be safe and well-tolerated. In addition, 5 and 10 mg were selected to capture the low-end of the exposure-response curve, and 20 and 50 mg were selected to define the exposure-response dynamic range. When the human PET data became available, it was found that the human brain occupancy observations were overall consistent with the model predictions (**Figure 4c**).

#### Human exposure-brain occupancy modeling analysis results

A total of 16 brain occupancy measures from 8 human subjects (single oral JNJ-54175446 doses of 5–300 mg) were included in the human exposure-occupancy modeling analysis. A sigmoidal  $E_{\max}$  model was developed and the parameter estimates are shown in **Table 2**. Compared

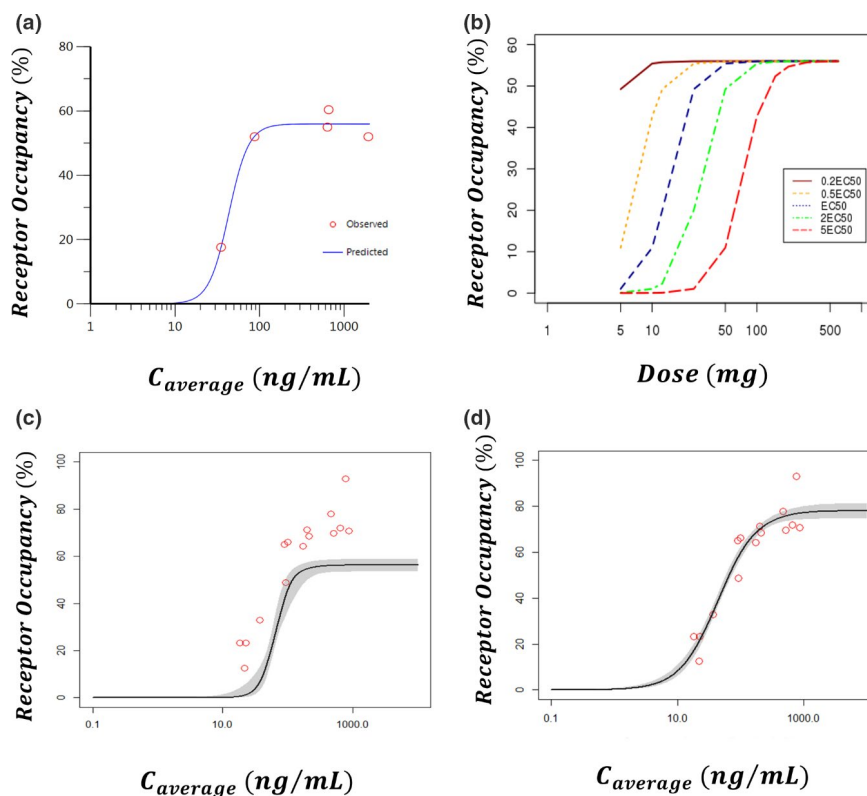
with the human  $EC_{50,RO}$  derived from monkeys (65.6 ng/mL), the model fitted  $EC_{50,RO}$  with clinical observations (44.3 ng/mL) is numerically lower but overall comparable (**Table 2**). The model fits indicated a less steep exposure-occupancy relationship ( $\gamma = 1.43$  in human vs. 3.71 in monkey) and a higher maximal occupancy in human compared with those in monkey ( $E_{\max} = 78.3\%$  in human vs. 56.0% in monkey; **Figure 4c,d**, **Table 2**).

**Figure 5** overlaid the observed and the simulated exposure-response relationships for the human brain P2X7 RO (blue) and the *ex vivo*-stimulated IL-1 $\beta$  release inhibition (red). With the increase of JNJ-54175446 plasma concentration, brain occupancy gradually increases and the *ex vivo*-stimulated IL-1 $\beta$  release decreases. The estimated human  $EC_{50,RO}$  for occupancy in the brain (44.3 ng/mL) is

**Table 2** Parameter estimates in the monkey and human exposure-response models for P2X7 receptor occupancy in the brain

Parameters	Description	Monkey estimates <sup>a</sup>	Human estimates <sup>a</sup>
$E_{\max}$ (%)	Maximal drug effect in RO	56.0 (4.41)	78.3 (1.78)
$EC_{50,RO}$ (ng/mL)	Drug concentration inducing 50% of maximal effect in RO	43.2 (9.02)	44.3 (4.25)
$\gamma$	Sigmoidal factor	3.71 (37.2)	1.43 (24.7)

RO, receptor occupancy.

<sup>a</sup>Mean (% relative standard error).


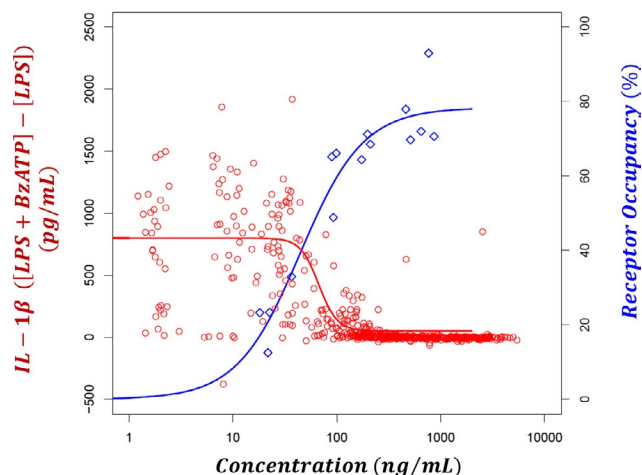
**Figure 4** Monkey and human exposure-response models for P2X7 receptor occupancy (RO) in the brain. (a) Observed vs. predicted brain RO in monkey. Open circles are the observed data and the line is the predicted. (b) Simulated dose-brain RO in human using translational pharmacokinetic/pharmacodynamic (PK/PD) model integrating human population PK and human exposure-brain occupancy relationship extrapolated from monkey PET. The concentration inducing 50% maximal drug effect for receptor occupancy ( $EC_{50,RO}$ ) is assumed to be 0.2-fold to 5-fold when compared with the derived human  $EC_{50,RO}$  from monkey. (c) Observed vs. predicted human brain RO using translational PK/PD model assuming a same unbound  $EC_{50,RO}$  between human and monkey. (d) Observed vs. predicted human brain RO using human exposure-response data from the clinical PET study. Open circles are the observed data and the line (area) is the predicted median (95% CI) trend.  $C_{average}$ , average plasma concentration over PET scan.

close to the  $EC_{50,IL1\beta}$  for IL-1 $\beta$  release inhibition in blood (67.0 ng/mL). These results confirmed the pharmacological activity of JNJ-54175446 as P2X7 receptor antagonist.

## DISCUSSION

In this study, we used a translational PK/PD modeling approach to guide dose selection for a human PET study of JNJ-54175446, a P2X7 receptor antagonist. Models were developed using data on monkey brain occupancy and drug exposures from a monkey PET study and early human clinical studies that provided data on drug exposures and

*ex vivo*-stimulated peripheral IL-1 $\beta$  release in human. The human dose-occupancy relationship was simulated using the exposure-occupancy model derived from monkeys assuming a similar unbound potency ( $EC_{50,RO} \times f_u$ ), together with the human population PK model. The model predicted occupancy data in human were largely consistent with the clinical observations, supporting the use of PET in monkeys as a tool to provide human-relevant occupancy information. This is further confirmed by the almost identical  $EC_{50,RO}$  estimates in human (44.3 ng/mL) and monkey (43.2 ng/mL). In a recent conference report, PET results had been collected for > 10 compounds and the  $EC_{50,RO}$



**Figure 5** Observed vs. predicted exposure-response relationships for P2X7 receptor occupancy in the brain (right y-axis, blue) and *ex vivo* provoked interleukin (IL)-1 $\beta$  release in the blood (left y-axis, red). Open circles and diamond are the individual observations for the IL-1 $\beta$  release and the brain occupancy, respectively. Lines are the model predicted median trends. BzATP, 3'-O-(4-benzoylbenzoyl)-ATP; LPS, lipopolysaccharide.

estimates were overall comparable between human and monkey for these compounds.<sup>14</sup> When comparing human with monkey in exposure-occupancy model fits, human tended to have a higher maximal occupancy and a less steep curve. This may reflect inherent physiological and/or pharmacological differences between human and monkey, driven by receptor binding kinetics.<sup>10,15</sup> However, due to the limited data, no definite conclusion could be drawn regarding species difference in current analysis. Nevertheless, our results indicate that monkey may be a predictive model for human PET target engagement and potentially informative for other drug development targets.

Of note, the estimated maximal occupancy was < 100% in monkey and human PET—which is expected. The basis of occupancy is comparing the estimation of the volume of distribution of the regional PET signal at baseline and after dosing. The PET signal includes specific (saturable/displaceable) and nonspecific binding. The subtraction of the signal reduces the contribution of nontarget binding but can never entirely “correct” for the nonspecific binding.

For the exposure-occupancy extrapolation from monkey to human, we assumed that human and monkey had a similar unbound potency. The assumption is based on the following considerations: (i) unbound drug concentration in plasma approximates pharmacologically active free concentration in the brain; and (ii) free but not bound drug binds to receptors in the brain. JNJ-54175446 is CNS-penetrating and its drug concentration in cerebrospinal fluid was comparable to the unbound plasma concentration.<sup>8</sup> Therefore, it is reasonable to extrapolate  $EC_{50,RO}$  from monkey to human after adjusting for differences in protein binding. Our derived human  $EC_{50,RO}$  was 65.6 ng/mL, similar to the potency for peripheral IL-1 $\beta$  release inhibition (67.0 ng/mL). This suggests that the functional effect of JNJ-54175446 on inhibiting the *ex vivo*-stimulated IL-1 $\beta$  release in blood cells may be a useful

surrogate for central occupancy, although the higher variability associated with the IL-1 $\beta$  release data vs. PET occupancy may limit such use (**Figure 5**). Improvement in IL-1 $\beta$  release bio-assay may help. Interestingly, comparable potencies between receptor binding and IL-1 $\beta$  release were also shown *in vitro*, with receptor binding affinity of 2.2 ng/mL ( $pK_i = 8.3$ ) and human whole blood IL-1 $\beta$  release half-maximal inhibitory concentration ( $IC_{50}$ ) of 3.5 ng/mL ( $pIC_{50} = 8.1$ ).<sup>1</sup>

It was later found that the model fitted human  $EC_{50,RO}$  (44.3 ng/mL) from clinical observations was closer to the monkey  $EC_{50,RO}$  (43.2 ng/mL) without fraction unbound adjustment. However, these data may be confounded by the overall low fraction unbound across species (11.2% in human and 17.0% in monkey) and not necessarily invalidate the assumption of similar unbound potency across species. For example, the analytical challenge associated with determining low free concentration may complicate the data interpretation. Nevertheless, fraction unbound correction for the projection of human  $EC_{50,RO}$  seems scientifically reasonable, although further work with additional agents may help confirm our hypothesis. Last, human PET  $EC_{50,RO}$  (44.3 ng/mL) was ~ 20-fold higher than *in vitro* receptor binding (2.2 ng/mL),<sup>1</sup> likely due to a more complex biological events and process *in vivo* (i.e., a myriad of potential interplay among drug, partitioning, target, and drug-target-complex).<sup>15</sup>

JNJ-54175446 demonstrated dose-dependent nonlinearity, with less than dose-proportional increase in exposure. To capture the dose-dependent PK, an empirical relative bioavailability ( $F_r$ ) was introduced to the population PK model. Dose-dependency was added on this parameter, where  $F_r$  decreased as doses increased. JNJ-54175446 tended to have a second peak in the absorption phase and  $T_{max}$  shifted to left as doses increased,<sup>8</sup> indicating atypical absorption due to reasons likely associated with its low solubility and high permeability properties (JNJ-54175446 is a Biopharmaceutics Classification System class II compound). This complex absorption was empirically described using a parallel zero-order and first-order absorption model with lag time. Zero-order absorption may occur due to low solubility and slow release from the “gut depot” and small fraction (~ 8%) of the oral JNJ-54175446 dose was absorbed in this route. The majority (~ 92%) of the dose was absorbed via first-order absorption as a result of intestinal absorption. Like most Biopharmaceutics Classification System class II compounds, JNJ-54175446 showed a positive food effect on its systemic exposure due to an increased solubility in fed state. The model-predicted food effects (60–70% increase in exposure with food) were consistent with the clinical observations of JNJ-54175446 that  $C_{max}$  and area under the curve (AUC) increased by 50–70% after a 50 mg dose and by 50% to 111% after a 300 mg dose, in the presence of a high-fat meal.<sup>8</sup>

The prediction of RO based on monkey data and using our translational PK/PD model mostly overlapped with the observed human occupancy data, indicating a successful pre-clinical to clinical translation for the JNJ-54175446 PET study. Using the translational PK/PD model, the initial dose for the



clinical PET study (150 mg) was accurately predicted to result in a close to maximal brain occupancy. Additionally, translational PK/PD model informed the way the study was designed and conducted; the continuous evaluation of occupancy data and the model-guided approach during the conduct of the study resulted in a decrease of the number of subjects that were included in the study. At the end, only 8 subjects were included in the trial, whereas 18 subjects were foreseen per protocol. Therefore, this modeling-aided strategy led to a more efficient PET study with fewer human subjects exposed for a shortened study duration (about 4 months ahead), and thereby reducing the total cost of the study.

The complex CNS biology, in combination with the lack of suitable animal models and clinically relevant biomarkers in these models, results in the less frequent use of translational PK/PD in neuroscience.<sup>16,17</sup> Noninvasive imaging techniques, such as PET, can generate useful and objective data on CNS drug effects in both preclinical species and human. It is thereby considered an ideal translational tool.<sup>18–20</sup> Our work may provide a foundation for a streamlined early clinical development for CNS drugs (i.e., use of *in silico* simulation of human brain occupancy based on monkey PET and translational modeling to improve human PET study design and efficiency). With accumulated information and increased confidence, such model-predicted occupancy in human might one day be able to substitute a clinical PET study, although the validity of this approach will need to be strengthened with drug candidates for different CNS targets before it can be accepted and applied in drug development. Of note, RO is not a direct measurement of efficacy *per se* and the occupancy required for clinical efficacy remains a challenge for CNS drug development.<sup>19</sup> Nevertheless, noninvasive PET imaging is a useful alternative for the lack of appropriate animal models within CNS. Monkey exposure-occupancy characterization would be critical in the implementation of this translational strategy and a well-designed monkey PET study covering the full dose range (not just high end) is essential.

**Supporting Information.** Supplementary information accompanies this paper on the *Clinical and Translational Science* website ([www.cts-journal.com](http://www.cts-journal.com)).

**Figure S1.** Additional goodness-of-fit plots for the final population pharmacokinetic model in human.

**Table S1.** Summary of human studies and data included in the modeling analyses.

**Table S2.** Key models during the human population pharmacokinetic model development.

**Table S3.** Simulated P2X7 receptor occupancy in the human brain.

**File S1.** Example model code and datasets.

**Acknowledgments.** The authors would like to thank Anna Katrin Szardenings for providing monkey PET study design information and data. The authors would also like to thank Marc Ceusters, Peter de Boer, and Anindya Bhattacharya for their helpful discussions.

**Funding.** This work was supported by Janssen Research & Development, LLC. and Pharmaceutical Companies of Johnson & Johnson.

**Conflict of Interest.** Y.X., M.X., P.R., A.H., M.S., P.N., and H.Z. are employees of Janssen Research & Development, LLC. at the time of the study and may own stock and/or stock options in the company.

**Author Contributions.** Y.X., M.X., and P.R. wrote the manuscript. Y.X., M.X., P.R., A.H. and M.S. designed the research. Y.X., M.X., and P.R. performed the research. Y.X., M.X., P.R., P.N., and H.Z. analyzed the data.

1. Letavic, M.A. *et al.* 4-Methyl-6,7-dihydro-4H-triazolo[4,5-c]pyridine-based P2X7 receptor antagonists: optimization of pharmacokinetic properties leading to the identification of a clinical candidate. *J. Med. Chem.* **60**, 4559–4572 (2017).
2. North, R.A. Molecular physiology of P2X receptor. *Physiol. Rev.* **82**, 1013–1067 (2002).
3. Collo, G., Neidhart, S., Kawashima, E., Kosco-Vilbois, M., North, R.A. & Buell, G. Tissue distribution of the P2X7 receptor. *Neuropharmacology* **36**, 1277–1283 (1997).
4. Ferrari, D. *et al.* The P2X7 receptor: a key player in IL-1 processing and release. *J. Immunol.* **176**, 3877–3883 (2006).
5. Wei, L. *et al.* ATP-activated P2X7 receptor in the pathophysiology of mood disorders and as an emerging target for the development of novel antidepressant therapeutics. *Neurosci. Biobehav. Rev.* **87**, 192–205 (2018).
6. Sperlágh, B. & Illes, P. P2X7 receptor: an emerging target in central nervous system diseases. *Trends. Pharmacol. Sci.* **35**, 537547 (2014).
7. Bhattacharya, A. Recent advances in CNS P2X7 physiology and pharmacology: focus on neuropsychiatric disorders. *Front. Pharmacol.* **9**, 30 (2018).
8. Timmers, M. *et al.* Clinical pharmacokinetics, pharmacodynamics, safety, and tolerability of JNJ-54175446, a brain permeable P2X7 antagonist, in a randomized single-ascending dose study in healthy participants. *J. Psychopharmacol.* **32**, 1341–1350 (2018).
9. Koole, M. *et al.* 18F-JNJ-64413739, a novel PET ligand for the p2x7 ion channel: radiation dosimetry, kinetic modeling, test-retest variability, and occupancy of the p2x7 antagonist JNJ-54175446. *J. Nucl. Med.* **60**, 683–690 (2019).
10. Zhang, Y. & Fox, G.B. PET imaging for receptor occupancy: meditations on calculation and simplification. *J. Biomed. Res.* **26**, 69–76 (2012).
11. Takano, A. *et al.* Guidelines to PET measurements of the target occupancy in the brain for drug development. *Eur. J. Nucl. Med. Mol. Imaging* **43**, 2255–2262 (2016).
12. Zhang, L., Beal, S.L. & Sheiner, L.B. Simultaneous vs. sequential analysis for population PK/PD data II: robustness of methods. *J. Pharmacokinetic. Pharmacodyn.* **30**, 405–416 (2003).
13. Kolb, H. *et al.* Preclinical evaluation and non-human primate receptor occupancy study of 18F-JNJ-64413739, a novel PET radioligand for P2X7 receptors. *J. Nucl. Med.* **60**, 1154–1159 (2019).
14. Hostetler, E. Translation from bench to bedside: PET tracers for use in neuroscience drug development. American Society for Clinical Pharmacology and Therapeutics 2018 Annual Meeting (2018). <[https://www.ascp.org/Portals/28/docs/Annual%20Meetings/2018%20Annual%20Meeting/Presentations/March%2023%202018/2018%20ASCP\\_Hostetler.pdf?ver=2018-04-12-194456-653](https://www.ascp.org/Portals/28/docs/Annual%20Meetings/2018%20Annual%20Meeting/Presentations/March%2023%202018/2018%20ASCP_Hostetler.pdf?ver=2018-04-12-194456-653)>. Accessed May 23, 2019.
15. Gabrielsson, J., Peletier, L.A. & Hjorth, S. Lost in translation: what's in an EC50? Innovative PK/PD reasoning in the drug development context. *Eur. J. Pharmacol.* **835**, 154–161 (2018).
16. Wong, H. *et al.* Translational pharmacokinetic-pharmacodynamic analysis in the pharmaceutical industry: an IQ Consortium PK-PD Discussion Group perspective. *Drug Discov. Today* **22**, 1447–1459 (2017).
17. Markou, A., Chiamulera, C., Geyer, M.A., Tricklebank, M. & Steckler, T. Removing obstacles in neuroscience drug discovery: the future path for animal models. *Neuropsychopharmacology* **34**, 74–89 (2009).
18. de Lange, E.C. & Hammarlund-Udenaes, M. Translational aspects of blood-brain barrier transport and central nervous system effects of drugs: from discovery to patients. *Clin. Pharmacol. Ther.* **97**, 380–394 (2015).
19. Grimwood, S. & Hartig, P.R. Target site occupancy: emerging generalizations from clinical and preclinical studies. *Pharmacol. Ther.* **122**, 281–301 (2009).
20. Fox, G.B., Chin, C.L., Luo, F., Day, M. & Cox, B.F. Translational neuroimaging of the CNS: novel pathways to drug development. *Mol. Interv.* **9**, 302–313 (2009).

© 2019 Janssen Research & Development LLC. *Clinical and Translational Science* published by Wiley Periodicals, Inc. on behalf of the American Society for Clinical Pharmacology and Therapeutics. This is an open access article under the terms of the Creative Commons Attribution-NonCommercial License, which permits use, distribution and reproduction in any medium, provided the original work is properly cited and is not used for commercial purposes.